14 Modelling Ca^{2+} Oscillations in Plants

Gerald Schönknecht*[1] and Claudia Bauer[2]

Abstract

To interpret the physiological functions of Ca^{2+} oscillations in plant cells, one has to understand how Ca^{2+} oscillations are generated and how they are modified by internal as well as external stimuli. Yet, oscillations result from nonlinear interactions of different components, which makes it impossible to intuitively predict how a certain stimulus might affect the frequency or amplitude of a Ca^{2+} oscillation. Usually, it is not even possible to explain why certain conditions result in Ca^{2+} oscillations whereas others do not. The only way to try to *explain* intracellular Ca^{2+} oscillations is by a mathematical model. Here, we give an introduction on how such a mathematical model can be derived. To start with, a general scheme of the Ca^{2+} fluxes in a plant cell is translated into a set of simple differential equations. Using Sr^{2+}-induced Ca^{2+} oscillations in the unicellular green alga *Eremosphaera viridis* as an example, this general scheme is then developed into a complete mathematical model. For this, the different Ca^{2+} fluxes driving the Ca^{2+} oscillations are discussed and, term by term, integrated into two coupled, nonlinear differential equations. Where possible, the mathematical description of the transmembrane Ca^{2+} fluxes is based on experimental results obtained with *E. viridis*. In some cases, assumptions based on models of Ca^{2+} oscillations in animal cells are introduced. A couple of simplifications are made to prevent the mathematical model from becoming excessively complex. Despite these limitations, the derived mathematical model qualitatively reproduces the dose dependence of frequency and amplitude of Sr^{2+}-induced Ca^{2+} oscillations in *E. viridis*. Finally, it is discussed how Ca^{2+} oscillations in other plant cells – such as Nod factor-induced Ca^{2+} oscillations in root hairs or Ca^{2+} oscillations in stomatal guard cells – might be described mathematically.

[1]Department of Botany, Oklahoma State University, Stillwater, OK 74078, USA
[2]Department of Biomedical Sciences, University of Sheffield, Western Bank, Sheffield S10 2TN, UK
*Corresponding author, e-mail: gerald.schoenknecht@okstate.edu

S. Mancuso and S. Shabala (Eds.)
Rhythms in Plants: Phenomenology, Mechanisms, and Adaptive Significance

14.1 Introduction

Being a result of nonlinear interactions among different components of a dynamic system, oscillations can hardly be understood intuitively. When it comes to sustained oscillations of the cytosolic free Ca^{2+} concentration – or Ca^{2+} oscillations for short – it is obvious that Ca^{2+} channels and Ca^{2+} pumps are involved (Berridge 1997; Hetherington and Brownlee 2004). Ca^{2+} channels mediate the influx of Ca^{2+} into the cytosol, from the exterior or from intracellular Ca^{2+} stores, and Ca^{2+} pumps mediate Ca^{2+} efflux from the cytosol, restoring cytosolic Ca^{2+} levels and refilling intracellular stores (Fig. 14.1). In such a generalised model, Ca^{2+} pumps can be understood as any type of membrane protein that transports Ca^{2+} against its electrochemical potential gradient. From a scheme such as that given in Fig. 14.1, however, it is impossible to predict under which conditions Ca^{2+} oscillations might be observed or not. Only a mathematical model can assess whether a certain system will show stable oscillations (i.e. limit cycle oscillations, see below) and under which conditions.

In animal cells, attempts to describe Ca^{2+} oscillations by mathematical models have formed an integral part of this research sphere almost from the very beginning (Meyer and Stryer 1988; Dupont et al. 1990), and the resulting mathematical models significantly contributed to a better understanding and the design of more refined experiments. By contrast, in plant cells we are

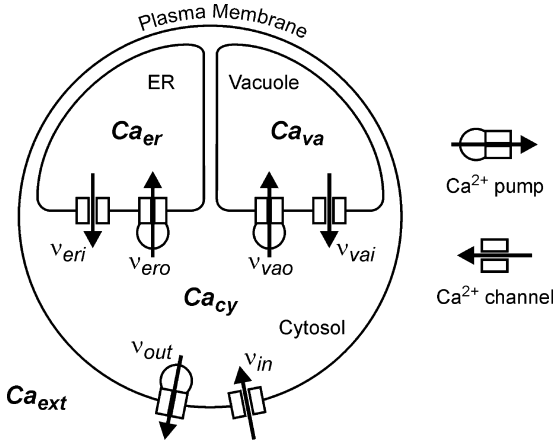

Fig. 14.1 General scheme of Ca^{2+} concentrations and Ca^{2+} fluxes in a plant cell. Ca_{cy}, Ca_{er}, Ca_{va} and Ca_{ext} are cytosolic, ER, vacuolar and external Ca^{2+} concentration respectively; v_{in} is influx of Ca^{2+} across the plasma membrane, v_{out} is transport of Ca^{2+} out of the cell, v_{eri} is influx of Ca^{2+} into the cytosol from the ER, v_{ero} is transport of Ca^{2+} out of the cytosol into the ER, v_{vai} is influx of Ca^{2+} into the cytosol from the vacuole, and v_{vao} is transport of Ca^{2+} out of the cytosol into the vacuole. Here, a Ca^{2+} pumps can be any membrane transport molecule that transports Ca^{2+} against its electrochemical potential gradient (i.e. out of the cytosol), and a Ca^{2+} channel can be any transport process that enables Ca^{2+} to cross the membrane down its electrochemical potential gradient

aware of only a single attempt to model Ca^{2+} oscillations mathematically (Bauer et al. 1998a). Oscillations in plant membrane potential resulting from fluctuations in membrane transporter activity have been described mathematically (Gradmann 2001; Shabala et al. 2006) but no mathematical models have been developed yet for Ca^{2+} oscillations observed in stomatal guard cells, pollen tubes or legume root hairs.

Mathematically, Ca^{2+} oscillations can be described at two different levels – on a molecular level or on a compartment level. On a molecular level, the spatial and temporal distribution of discrete Ca^{2+} ions is calculated by stochastic algorithms (Kraus et al. 1996; Kummer et al. 2005). On a compartment level, continuous concentrations are calculated by integrating differential equations. This latter deterministic approach assumes homogeneous concentration within each compartment, and is mathematically much simpler than that for stochastic models. In small compartments, however, particle numbers may become so low that spatial fluctuations can no longer be ignored, and the assumption of homogeneous concentrations is no longer valid. For example, a compartment of 1 μm^3 with a free Ca^{2+} concentration of 100 nM contains only 60 free Ca^{2+} cations. Compared to this, the cytosolic volume of an *Arabidopsis* guard cell is in the order of 10 μm^3, and cell organelles may have volumes of less than 1 μm^3. Even though there are indications that stochastic effects might be relevant at physiological Ca^{2+} concentrations (Kummer et al. 2005), to date most mathematical models of Ca^{2+} oscillations are based on deterministic models (Schuster et al. 2002). The following example illustrating how a mathematical model of Ca^{2+} oscillations can be developed is based on experiments performed with the unicellular green alga *Eremosphaera viridis*. The spherical cells of *E. viridis* have a diameter of about 150 µm, resulting in compartment volumes that most likely justify a deterministic approach.

For the benefit of the reader, in the following are listed the definitions of some key abbreviations used in this chapter. CICR, Ca^{2+}-induced Ca^{2+} release; CPA, cyclopiazonic acid; DBHQ, 2,5-di-tert-butylhydroquinone; IP_3, inositol 1,4,5-trisphosphate.

14.2 Developing a Mathematical Model

To understand how a mathematical model of Ca^{2+} oscillations can be developed, let us start with the general scheme in Fig. 14.1, summarizing Ca^{2+} concentrations and Ca^{2+} fluxes in a plant cell. For this general model, the differential equations describing changes of intracellular Ca^{2+} concentrations can directly be written as:

$$\frac{\mathrm{d}}{\mathrm{d}t} Ca_{\mathrm{cy}} = \nu_{\mathrm{in}} - \nu_{\mathrm{out}} + \nu_{\mathrm{eri}} - \nu_{\mathrm{ero}} + \nu_{\mathrm{vai}} - \nu_{\mathrm{vao}} \tag{14.1}$$

$$\frac{\mathrm{d}}{\mathrm{d}t} Ca_{\mathrm{er}} = \rho_{\mathrm{er}} (\nu_{\mathrm{ero}} - \nu_{\mathrm{eri}}) \tag{14.2}$$

$$\frac{\mathrm{d}}{\mathrm{d}t} Ca_{\mathrm{va}} = \rho_{\mathrm{va}} (\nu_{\mathrm{vao}} - \nu_{\mathrm{vai}}) \tag{14.3}$$

where Ca_{cy}, Ca_{er}, Ca_{va} and Ca_{ext} are cytosolic, ER, vacuolar and external Ca^{2+} concentration respectively, ν_{in} is influx of Ca^{2+} across the plasma membrane, ν_{out} is transport of Ca^{2+} out of the cell, ν_{eri} is influx of Ca^{2+} into the cytosol from the ER, ν_{ero} is transport of Ca^{2+} out of the cytosol into the ER, ν_{vai} is influx of Ca^{2+} into the cytosol from the vacuole, ν_{vao} is transport of Ca^{2+} out of the cytosol into the vacuole, and ρ_{er} and ρ_{va} are the cytosol/ER and cytosol/vacuole volume ratios respectively. Ca_{ext}, the external Ca^{2+} concentration, is usually assumed to be constant. Throughout this chapter, italic symbols of substances are used for concentrations, e.g. $[Ca^{2+}]_{\mathrm{cy}} \rightarrow Ca_{\mathrm{cy}}$.

Obviously, the general model presented in Fig. 14.1 and Eqs. (14.1) to (14.3) is grossly simplified. It contains only two intracellular Ca^{2+} stores, does not include any signalling components such as IP_3, and neither is Ca^{2+} buffering considered. It would indeed be possible to add additional Ca^{2+} stores but, as demonstrated below, a single Ca^{2+} store is sufficient for the generation and maintenance of stable Ca^{2+} oscillations. Signalling components such as IP_3, which release Ca^{2+} from internal stores, are an important component of most models for Ca^{2+} oscillation in animal cells (Schuster et al. 2002). In a less complex case, a certain concentration of IP_3 promotes Ca^{2+} release from internal stores into the cytoplasm. In the general scheme given above, this would simply cause an increase in ν_{eri} and/or ν_{vai}. In more complex cases, IP_3 (the IP_3 concentration) may be a separate variable, and IP_3 dynamics is described by a differential equation. Ca^{2+} binding by buffers can modulate Ca^{2+} oscillations, and mathematical models have been developed that describe Ca^{2+} binding by a separate variable/differential equation. To keep things simple, we stay with the general model presented in Fig. 14.1 and Eqs. (14.1) to (14.3). It contains (almost) everything needed for stable cytosolic Ca^{2+} oscillations.

To start with, we consider an example of Ca^{2+} oscillations observed in a plant cell. When the unicellular green alga *E. viridis* is perfused with a bath solution containing Sr^{2+} (0.1 mM or more) or caffeine (1 mM or more), cytosolic Ca^{2+} oscillations are observed (Bauer et al. 1997). Our group performed a pharmacological characterization of these Ca^{2+} oscillations to elucidate the molecular mechanisms of Ca^{2+} oscillations in a plant cell. Based on experimental results, we were able to develop a mathematical model that describes Sr^{2+}-induced Ca^{2+} oscillations in *E. viridis* (Bauer et al. 1998a). The principal findings of the pharmacological experiments are summarized in Fig. 14.2. In the following sections, these results are used to develop Eqs. (14.1) and (14.2) into a mathematical model for Sr^{2+}-induced Ca^{2+} oscillations.

We begin at the plasma membrane (ν_{in} and ν_{out} in Fig. 14.1). Models of Ca^{2+} oscillations can be divided into two groups – those with constant total cellular Ca^{2+} content ($\nu_{\mathrm{in}}=0$, $\nu_{\mathrm{out}}=0$) and those with changing total cellular

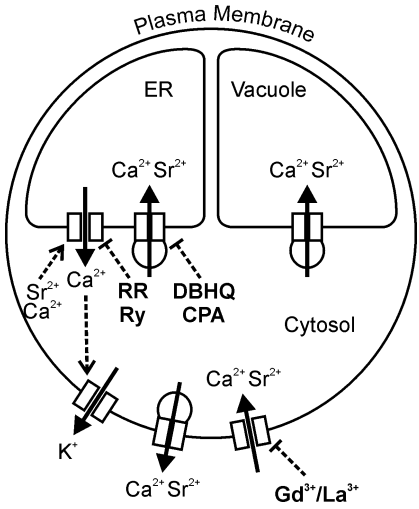

Fig. 14.2 Model for Sr^{2+}-induced Ca^{2+} oscillations in the unicellular green alga *Eremosphaera viridis*. Sr^{2+} enters the cell via plasma membrane cation channels that are blocked by Gd^{3+} or La^{3+}. Most of the Sr^{2+} taken up into the cell is compartmentalized into the vacuole. Ca^{2+} (and Sr^{2+}?) is transported into the ER by Ca^{2+}-ATPases that are specifically blocked by DCBQ and CPA. In the cytosol, Ca^{2+} and Sr^{2+} induce a Ca^{2+}-induced Ca^{2+} release (CICR) from the ER. The ER Ca^{2+} channel is blocked by either ruthenium red (RR) or ryanodine (Ry). Increasing cytosolic Ca^{2+} causes the opening of plasma membrane K^+ channels, resulting in a hyperpolarization (Bauer et al. 1998a)

Ca^{2+} content, due to Ca^{2+} fluxes across the plasma membrane. To test for the importance of Ca^{2+} uptake into the cell, we applied La^{3+} and Gd^{3+} during Sr^{2+}-induced or caffeine-induced Ca^{2+} oscillations. Both trivalent cations rapidly and reversibly blocked Ca^{2+} oscillations induced by either Sr^{2+} or caffeine (Bauer et al. 1997, 1998a). Cation uptake measurements (by ICP-AES analysis of cell sap) showed that neither La^{3+} nor Gd^{3+} reached detectable intracellular concentrations. Therefore, La^{3+} and Gd^{3+} most likely inhibited Ca^{2+} oscillations by blocking Ca^{2+} influx across the plasma membrane, indicating the necessity of Ca^{2+} uptake into the cell for sustained Ca^{2+} oscillations.

Ca^{2+} influx across the plasma membrane, v_{in}, depends on Ca_{ext} and the electrochemical potential difference for Ca^{2+}. Ca_{ext} was constant under our experimental conditions and, therefore, does not need further consideration. The electrochemical potential gradient for Ca^{2+}, however, does change during Ca^{2+} oscillations. Increasing Ca_{cy} during a Ca^{2+} spike decreases the chemical potential difference for Ca^{2+} across the plasma membrane. Moreover, Ca^{2+} oscillations in *E. viridis* have been shown to be accompanied by membrane potential oscillations, caused by the Ca^{2+}-dependent opening of plasma membrane K^+ channels (Bauer et al. 1998b). Each cytosolic Ca^{2+} spike induces a hyperpolarization increasing the electrical potential difference. How do these

opposing changes in chemical and electrical driving force affect Ca^{2+} influx into the cell (v_{in})? To answer this question, we systematically varied the electrical driving force, i.e. the membrane potential, during Sr^{2+}-induced Ca^{2+} oscillations. When the external K^+ concentration is increased, the membrane potential of *E. viridis* becomes less negative and the transient hyperpolarizations (at 0.1 mM external K^+) accompanying Ca^{2+} spikes change into transient depolarizations (at 100 mM external K^+). Furthermore, cytosolic Ca^{2+} oscillations are not significantly altered by the membrane potential change induced by increasing external K^+ (Bauer et al. 1998a). Even though Ca^{2+} oscillations in *E. viridis* are accompanied by membrane potential oscillations, the membrane potential does not seem to have a large effect on the Ca^{2+} oscillations. For an initial, simplified mathematical model, therefore, we assumed v_{in}=const.

If there is Ca^{2+} uptake into the cell, then there has to be Ca^{2+} transport out of the cell to prevent Ca^{2+} from accumulating over time. For the mathematical model, we simply assume the activity of a plasma membrane Ca^{2+}-ATPase that pumps Ca^{2+} out of the cell with a rate proportional to the cytosolic concentration, Ca_{cy} ($v_{out}=k_{out}\cdot Ca_{cy}$). This assumption, again, is a simplification, ignoring saturation of transport rates at high substrate concentrations, as described by Michaelis-Menten-type transport kinetics. Yet, many transporters operate at substrate concentrations below their K_m (Michaelis constant) values, resulting in an effectively linear relationship between transport rate and substrate concentration. Even if a linear relationship is not exactly given, this approximation seems to be justified for qualitative description.

To describe self-sustained oscillations by a system of differential equations, at least two variables are needed (Stucki and Somogyi 1994). In the case of Ca^{2+} fluxes between the cytosol and the intracellular Ca^{2+} stores (v_{eri}, v_{ero}, v_{vai}, v_{vao}), one of these variables is obviously Ca_{cy}, the cytosolic Ca^{2+} concentration; the other variable might be the Ca^{2+} concentration inside an intracellular Ca^{2+} store, Ca_{er} or Ca_{va} (in the general model given in Fig. 14.1 and Eqs. 14.1 to 14.3). Alternatively, the other variable might be IP_3 (or the changing sensitivity of IP_3 receptors), or the number of Ca^{2+} buffer groups binding Ca^{2+}, or the membrane potential (Schuster et al. 2002). More complex models may contain more than two variables.

In the case of Sr^{2+}-induced (or caffeine-induced) Ca^{2+} oscillations in *E. viridis*, there is experimental evidence that the Ca^{2+} concentration of an intracellular store – most likely the ER (Ca_{er}) – is such another variable. Why the ER and not the vacuole? The Ca^{2+} content of the vacuole is probably too high to show significant changes during cytosolic Ca^{2+} oscillations. In *E. viridis*, the vacuolar free Ca^{2+} concentration is 200 µM, compared to 160 nM in the cytosol (Bethmann et al. 1995). Based on a roughly tenfold larger volume of the vacuole, the total Ca^{2+} content of the vacuole would be four orders of magnitude higher than that of the cytosol – assuming comparable Ca^{2+} buffer capacities. Even if the cytosolic Ca^{2+} buffer capacity were 100 times larger than the vacuolar buffer capacity, which is not likely to be the case (Schönknecht

and Bethmann 1998), a Ca^{2+} release from the vacuole that increases the cytosolic free Ca^{2+} concentration from 160 nm to 1.6 µM would not result in a significant change of the free vacuolar Ca^{2+} concentration. It is the large amount of Ca^{2+} accumulated inside the vacuole that makes is rather unlikely that cytosolic Ca^{2+} oscillations are accompanied by vacuolar Ca^{2+} oscillations, thus ruling out the vacuolar Ca^{2+} concentration (Ca_{va}) as second variable for the mathematical model.

In line with these quantitative considerations, our experimental evidence points to a rather small intracellular Ca^{2+} store driving Sr^{2+}-induced (and caffeine-induced) Ca^{2+} oscillations in *E. viridis*. Application of the ER Ca^{2+}-ATPase blocker DBHQ or CPA (10 µM in each case) stops Sr^{2+}-induced Ca^{2+} oscillations within a few minutes. The baseline Ca_{cy} level and Sr^{2+} uptake and compartmentalization are not affected by DBHQ, indicating that Ca^{2+} and Sr^{2+} homeostasis is still maintained by Ca^{2+} pumps not inhibited by DBHQ (Bauer et al. 1998a). DBHQ and CPA have been shown to act specifically on ER Ca^{2+}-ATPases both in animal (Inesi and Sagara 1994) and plant cells (Logan and Venis 1995; Hwang et al. 1997; Liang et al. 1997). As evident from Fig. 14.2, blocking ER Ca^{2+}-ATPases by DBHQ or CPA prevents the reuptake of Ca^{2+} into the ER, resulting in a depletion of the intracellular Ca^{2+} store that is needed to drive the Ca^{2+} oscillations. For the mathematical model, we assume the transport rate of the ER Ca^{2+}-ATPase to be proportional to the cytosolic Ca^{2+} concentration ($v_{ero}=k_{ero}\cdot Ca_{cy}$) – as we assume for the plasma membrane Ca^{2+}-ATPase, too (v_{out}, see above).

Finally, we need a mathematical term describing the Ca^{2+} efflux from the intracellular store (v_{eri}) that increases Ca_{cy} during Ca^{2+} oscillations. Most Ca^{2+} oscillations investigated in animal cells seem to be driven by intracellular Ca^{2+} release via IP_3 receptors (Schuster et al. 2002). TMB_8 (3,4,5-trimethoxybenzoic acid 8-diethylaminooctyl ester), an inhibitor of IP_3-induced Ca^{2+} release in *E. viridis* (Förster 1990), does not block Sr^{2+}-induced Ca^{2+} oscillations at concentrations of up to 200 µM, indicating that IP_3 receptors are not involved. In animal cells, caffeine and Sr^{2+} are known to induce Ca^{2+} release from the ER (and sarcoplasmic reticulum) via the ryanodine receptor (Meissner 1994). In *E. viridis*, both Sr^{2+} and caffeine induce identical Ca^{2+} oscillations (Bauer et al. 1997). Ruthenium red (Ma 1993) and ryanodine (Smith et al. 1988) are known to be specific for the ryanodine receptor in animal cells (Ehrlich et al. 1994), and have been shown to block Ca^{2+} release in plant cells (Allen et al. 1995; Muir and Sanders 1996). When microinjected into *E. viridis*, both inhibitors block Sr^{2+}-induced (and caffeine-induced) membrane potential oscillations accompanying Ca^{2+} oscillations, whereas membrane potential changes induced by other changes (such as darkening) are not affected (Bauer et al. 1998a). This indicates that ruthenium red and ryanodine specifically block Sr^{2+}-induced Ca^{2+} release from the ER but not the Ca^{2+} release from chloroplasts after darkening. Summarizing, in *E. viridis* cytosolic Sr^{2+} seems to induce Ca^{2+} release from the ER by activating a ryanodine receptor type of Ca^{2+} channel (see Fig. 14.2).

How can this component, the Sr^{2+}-induced Ca^{2+} release from the ER (v_{eri}), be mathematically described to complete the mathematical model of Sr^{2+}-induced Ca^{2+} oscillations in *E. viridis*? Very little is known about ryanodine receptor-type Ca^{2+} channels in plants. At this point, to achieve a qualitative description of the Sr^{2+}-induced Ca^{2+} release in *E. viridis*, one has to rely on data from animal cells. Ryanodine receptors, similarly to IP_3 receptors, show so-called Ca^{2+}-induced Ca^{2+} release (CICR). This means that a relatively small initial increase in Ca_{cy} activates ryanodine receptors, resulting in Ca^{2+} release and, thus, a further increase of Ca_{cy}. Almost all models of Ca^{2+} oscillations with only two variables are based on CICR as a positive feedback element (Schuster et al. 2002). This is important, since another requirement for stable oscillations is feedback. At least one feedback step has to connect the variables. This feedback is usually positive, since negative feedback loops in most cases act as stabilizing elements, returning the variables to their steady-state values preventing oscillations (Stucki and Somogyi 1994).

CICR is a nonlinear process and, in mathematical models of Ca^{2+} oscillations, cooperative Ca^{2+} binding (with Hill coefficients of two or higher) to the ryanodine receptor or IP_3 receptor is often assumed (Somogyi and Stucki 1991; Schuster et al. 2002). For isolated ryanodine receptor complexes of the sacroplasmic reticulum, a positive cooperativity for Ca^{2+}-dependent channel gating has been shown (Meissner et al. 1986; Pessah et al. 1987). The positive nonlinear feedback by CICR is a central element of many Ca^{2+} oscillation models (Berridge 1990; Dupont and Goldbeter 1993; Bootman et al. 1996). Why is nonlinear feedback important? A further requirement for stable oscillations is 'sufficient total nonlinearity' (Stucki and Somogyi 1994), as a system of linear kinetics will not give rise to stable oscillations. In most models, it is the feedback element that is assumed to be nonlinear. This nonlinearity can come from Michaelis-Menten-type kinetics, positive cooperativity, etc. (Stucki and Somogyi 1994). In line with existing models of Ca^{2+} oscillations and what is known about the ryanodine receptor in animal cells, we assume that Ca^{2+}-induced Ca^{2+} release from the ER (v_{eri}) in *E. viridis* is based on cooperative Ca^{2+} binding. This is mathematically formulated as:

$$v_{eri} = k_{eri} \cdot \frac{Ca_{cy}^{\,n}}{K^n + Ca_{cy}^{\,n}} \cdot (Ca_{er} - Ca_{cy}) \qquad (14.4)$$

where k_{eri} is the rate constant for Ca^{2+} release by the ryanodine receptor, K is the affinity constant for Ca^{2+} binding (half maximum binding), n is the Hill coefficient, and all other symbols are as in the general model given in Fig. 14.1 and Eqs. (14.1) to (14.3). Equation (14.4) describes a Ca^{2+} channel (k_{eri}) that is modulated in a cooperative manner (K, n) by cytosolic Ca^{2+} (Ca_{cy}) while the difference in Ca^{2+} concentration between ER and cytosol (Ca_{er}-Ca_{cy}) drives the Ca^{2+} flux (v_{eri}).

Next, Sr^{2+} has to be included. It is known that Sr^{2+}, similarly to Ca^{2+} (and caffeine), gates the ryanodine receptor open, triggering Ca^{2+} release

(Meissner 1994). For Sr^{2+}-induced Ca^{2+} oscillations in *E. viridis*, it is therefore assumed that there is both a Ca^{2+}-induced Ca^{2+} release and a Sr^{2+}-induced Ca^{2+} release from the ER via a ryanodine receptor-type Ca^{2+} channel. Accordingly, Eq. (14.4) is extended to:

$$\nu_{\mathrm{eri}} = k_{\mathrm{eri}} \cdot \frac{(Ca_{\mathrm{cy}} + Sr_{\mathrm{cy}})^n}{K^n + (Ca_{\mathrm{cy}} + Sr_{\mathrm{cy}})^n} \cdot (Ca_{\mathrm{er}} - Ca_{\mathrm{cy}}) \tag{14.5}$$

where Sr_{cy} is the cytosolic Sr^{2+} concentration. For simplicity, the same affinity constant, K, and Hill coefficient, n, are assumed for Ca^{2+} and Sr^{2+}.

Equation (14.5) describes a sigmoid function with a very low Ca^{2+} flux, ν_{eri}, in the absence of Sr^{2+} (Sr_{cy}=0) and at low Ca_{cy} (<200 nM at rest). However, we have experimental evidence that there is a considerable Ca^{2+} efflux from the ER even in the absence of Sr^{2+} and at low Ca_{cy}. Incubation of *E. viridis* with the ER Ca^{2+}-ATPase blocker DBHQ or CPA for more than 5 min completely inhibits Sr^{2+}-induced Ca^{2+} oscillations (Bauer et al. 1998a). Similarly to animal cells (Kass et al. 1989; Demaurex et al. 1992), there probably is a continuous efflux of Ca^{2+} from the ER in *E. viridis* and, when the compensating Ca^{2+} uptake by the ER Ca^{2+}-ATPase is inhibited, this results in store depletion preventing Ca^{2+} oscillations. To account for this continuous Ca^{2+} efflux, an additional 'leak' term, $k_{\mathrm{erL}} \cdot (Ca_{\mathrm{er}} - Ca_{\mathrm{cy}})$, is introduced that describes a Ca^{2+} efflux proportional to the driving force – the difference in Ca^{2+} concentration between the ER and cytosol ($Ca_{\mathrm{er}} - Ca_{\mathrm{cy}}$). This leak term is added to Eq. (14.5) to obtain a complete description of the Ca^{2+} efflux from the ER (ν_{eri}):

$$\nu_{\mathrm{eri}} = \left(k_{\mathrm{erL}} + k_{\mathrm{eri}} \cdot \frac{\left(Ca_{\mathrm{cy}} + Sr_{\mathrm{cy}}\right)^n}{K^n + \left(Ca_{\mathrm{cy}} + Sr_{\mathrm{cy}}\right)^n} \right) \cdot \left(Ca_{\mathrm{er}} - Ca_{\mathrm{cy}}\right) \tag{14.6}$$

where k_{erL} is the rate constant (proportionality factor) for the Ca^{2+} leak from the ER. Having discussed all Ca^{2+} fluxes that are summarized in the general model in Fig. 14.1 and Eqs. (14.1) to (14.3), ν_{out}, ν_{eri} and ν_{ero} can now be substituted, converting Eqs. (14.1) and (14.2) into:

$$\begin{cases} \dfrac{\mathrm{d}}{\mathrm{d}t} Ca_{\mathrm{cy}} = \nu_{\mathrm{in}} - \left(k_{\mathrm{out}} + k_{\mathrm{ero}}\right) \cdot Ca_{\mathrm{cy}} + \left(k_{\mathrm{erL}} + k_{\mathrm{eri}} \cdot \dfrac{\left(Ca_{\mathrm{cy}} + Sr_{\mathrm{cy}}\right)^n}{K^n + \left(Ca_{\mathrm{cy}} + Sr_{\mathrm{cy}}\right)^n} \right) \cdot \\ \qquad \left(Ca_{\mathrm{er}} - Ca_{\mathrm{cy}}\right) \\ \dfrac{\mathrm{d}}{\mathrm{d}t} Ca_{\mathrm{er}} = \rho_{\mathrm{er}} \left(k_{\mathrm{ero}} \cdot Ca_{\mathrm{cy}} - \left(k_{\mathrm{erL}} + k_{\mathrm{eri}} \cdot \dfrac{(Ca_{\mathrm{cy}} + Sr_{\mathrm{cy}})^n}{K^n + (Ca_{\mathrm{cy}} + Sr_{\mathrm{cy}})^n} \right) \cdot \left(Ca_{\mathrm{er}} - Ca_{\mathrm{cy}}\right) \right) \end{cases} \tag{14.7}$$

Figure 14.3 gives a scheme explaining Eq. (14.7). Cytosolic Sr^{2+} initializes Ca^{2+}/Sr^{2+}-induced Ca^{2+} release from the ER. Due to a nonlinear positive feedback (Eq. 14.5), this results in a rapid, autocatalytic increase of Ca_{cy}.

Decreasing Ca_{er} and increasing Ca_{cy} slow down Ca^{2+} release. The ER Ca^{2+}-ATPase (k_{ero}) refills the ER Ca^{2+} store ($Ca_{er}\uparrow$) and, together with the plasma membrane Ca^{2+}-ATPase (k_{out}), causes Ca_{cy} to decrease to the baseline level once again.

14.3 Discussion of the Model

A comparison of Figs. 14.1 and 14.2 with Fig. 14.3 shows that the vacuole is not included in the mathematical model. The quantitative considerations given above indicate that Ca_{va} is unlikely to oscillate in *E. viridis*. In addition, there is no experimental evidence that Ca^{2+} fluxes between the cytosol and the vacuole play a significant role for Sr^{2+}-induced Ca^{2+} oscillations in *E. viridis*. It therefore seems justified to omit Ca_{va}, v_{vai} and v_{vao} in the mathematical model (Eq. 14.7).

The differential equations shown in Eq. (14.7) can not be integrated analytically but only numerically, i.e. step by step, starting with a certain set of

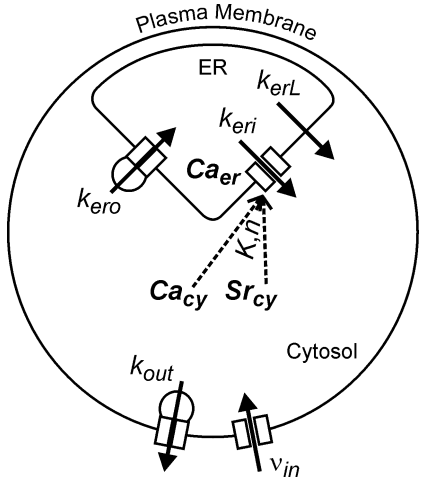

Fig. 14.3 Model of the Ca^{2+} oscillator described by Eq. (14.7). All parameters and variables used in Eq. (14.7) for the mathematical model of Sr^{2+}-induced Ca^{2+} oscillations in *E. viridis* are depicted in a schematic way. There is a constant Ca^{2+} influx from the external medium (v_{in}), and this constant Ca^{2+} influx is compensated by a plasma membrane Ca^{2+}-ATPase that pumps Ca^{2+} out of the cytosol (k_{out}). The ER is the intracellular Ca^{2+} store driving the Ca^{2+} oscillations, and Ca_{er} – in addition to Ca_{cy} – is the second variable changing over time in this model. There is a continuous efflux of Ca^{2+} from the ER due to a leak (k_{erL}). Sr^{2+} most likely enters the cell by the same pathway as does Ca^{2+}, and a Ca^{2+}/Sr^{2+}-induced Ca^{2+} release from the ER (k_{eri}) causes the rapid increase of Ca_{cy} initializing Ca^{2+} oscillations. The binding of Ca^{2+} and Sr^{2+} to the ER Ca^{2+} release channel (ryanodine receptor type) is assumed to be cooperative (K, n). The Ca^{2+} store is refilled by a ER Ca^{2+}-ATPase (k_{ero})

start values, $Ca_{cy}(t=0)$ and $Ca_{er}(t=0)$. This can be conveniently performed using Mathematica© (Wolfram Research Inc., Champaign, IL) or any other comparable software package. Figure 14.4 compares Sr^{2+}-induced Ca^{2+} oscillations measured in *E. viridis* (Fig. 14.4a) with Ca^{2+} oscillations calculated by numerically solving Eq. (14.7), the latter shown in Fig. 14.4b. In Fig. 14.4b, the following parameter set was used: $v_{in}=1$, $k_{out}=1$, $k_{ero}=2$, $k_{erL}=0.05$, $k_{eri}=1.2$, $K=2.5$, $n=4$, $Sr_{cy}=0.1$, $\rho_{er}=1$, with $Ca_{cy}(t=0)=0.2$ and $Ca_{er}(t=0)=24$ as start values. The same parameter set, but with $Sr_{cy}=0$, does not result in oscillations – as should be the case for Sr^{2+}-induced Ca^{2+} oscillations.

As a simplification, no units are given for the parameter values used to solve Eq. (14.7); as a result, the axes for the calculated Ca^{2+} oscillations (Fig. 14.4 b and c) are given in arbitrary units. For a first qualitative evaluation, this seems justified. For a more detailed simulation yielding time axes in seconds

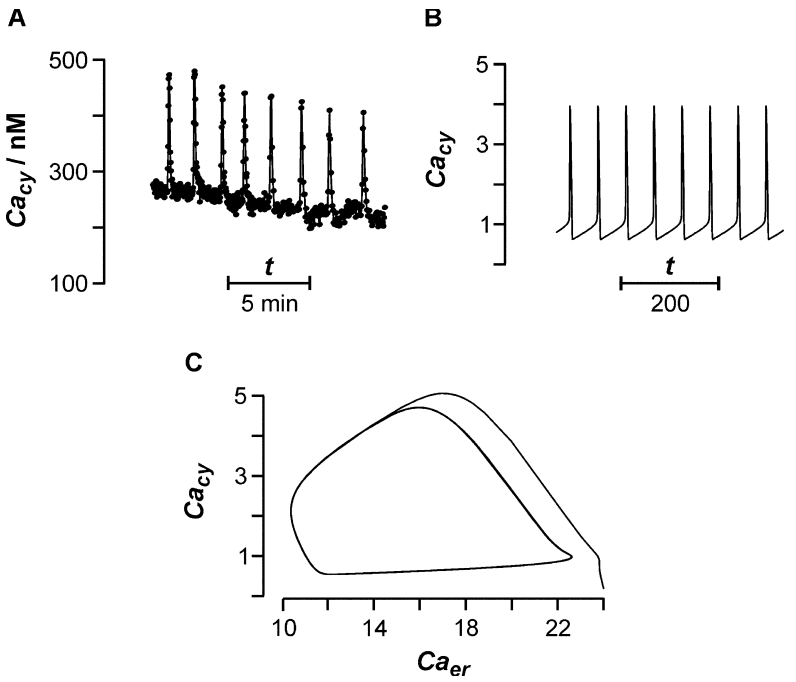

Fig. 14.4 Measured and calculated Ca^{2+} oscillations. **a** Sr^{2+}-induced Ca^{2+} oscillations measured in a single *E. viridis* cell in the presence of 1 mM $SrCl_2$ in the external medium. Ca_{cy} was measured at a sampling frequency of 1/3 s^{-1} after mechanical microinjection of the fluorescent Ca^{2+}-sensitive dye fura-2-dextran. **b** Sr^{2+}-induced Ca^{2+} oscillation calculated by numerical integration of Eq. (14.7), using the following parameter set: $v_{in}=1$, $k_{out}=1$, $k_{ero}=2$, $k_{erL}=0.05$, $k_{eri}=1.2$, $K=2.5$, $n=4$, $Sr_{cy}=0.1$, $\rho_{er}=1$, and with $Ca_{cy}(t=0)=0.2$ and $Ca_{er}(t=0)=24$ as start values. **c** Calculated values of Ca_{cy} are plotted against calculated values for Ca_{er}, displaying the so-called limit cycle. Starting at $Ca_{cy}(t=0)=0.2$ and $Ca_{er}(t=0)=24$, the two variables quickly approach the limit cycle. For sake of simplicity, no units are given and the axes are given in arbitrary units for the calculated Ca^{2+} oscillation (in **b** and **c**; see text)

and Ca_{cy}-axes in nM, additional parameters would have to be introduced – such as the Ca^{2+} buffer capacity – and reasonable values for most parameters would have to be available. However, for most of the rate constants, affinities, volumes, buffer capacities, etc. needed for a more detailed model, no established values exist. For the time being, therefore, more detailed models with additional parameters are more likely to introduce additional uncertainty than to achieve higher accuracy. To solve the mathematical functions developed here (Eq. 14.7), most parameters were given values close to 1. The activity of the ER Ca^{2+}-ATPase (k_{ero}=2) is assumed to be twice as high as the activity of the plasma membrane ATPase (k_{out}=1), and the leak releasing Ca^{2+} from the ER (k_{erL}=0.05) is assumed to have a much lower rate constant than that for the Sr^{2+}/Ca^{2+}-induced Ca^{2+} release (k_{eri}=1.2) – all these seem to be reasonable assumptions.

In Fig. 14.4c, Ca_{cy} is plotted against Ca_{er}. The closed curve in this plot is referred to as limit cycle. From their start values, the two variables ($Ca_{cy}(t=0)$=0.2, $Ca_{er}(t=0)$=24) quickly approach this limit cycle and then cycle in a fixed orbit. For stable oscillations, the size and shape of the limit cycle depend on the parameter set used but not on the start values of the two variables. Regardless of the start values, the oscillation will always culminate in exactly the same limit cycle (Stucki and Somogyi 1994). Stable oscillations are therefore also referred to as limit cycle oscillations.

Starting with the parameter set used in Fig. 14.4, one can now change the values for different parameters and observe how this affects the calculated oscillations. During the investigation of Sr^{2+}-induced Ca^{2+} oscillations in *E. viridis*, it had been observed that an increase in external Sr^{2+} concentrations resulted in faster oscillations with smaller amplitudes (Bauer et al. 1998a); analogous observations were made when different amounts of Sr^{2+} were injected directly into the algal cell. Changing the value for Sr_{cy} in Eq. (14.7) results in a similar behaviour for the calculated oscillations. Keeping all other parameters as in Fig. 14.4, no oscillations are observed below Sr_{cy}=0.08. Increasing Sr_{cy} results in an increasing frequency, from a wavelength of λ=64 at Sr_{cy}=0.08 to λ=14.3 at Sr_{cy}=0.54. Amplitudes start decreasing already at Sr_{cy}>0.11 and, at about Sr_{cy}=0.5, amplitudes become very small, resulting in 'saw tooth' shape oscillations. At Sr_{cy}=0.55, no oscillation occurs. The dose dependence of frequency and amplitude of Sr^{2+}-induced Ca^{2+} oscillations recorded in *E. viridis* can qualitatively be reproduced by the mathematical model described by Eq. (14.7).

This good correspondence between experimental data and the mathematical model does not, of course, prove that the model is correct. Nonetheless, it demonstrates that even a highly simplified model is sufficient to reflect the Sr^{2+} dose dependence observed. The assumption of a constant Sr_{cy} itself is also a simplification and, in a more realistic model, the Sr^{2+} concentration in the cytoplasm (Sr_{cy}) and in the ER (Sr_{er}) could be treated as variables. Ultimately, this would result in a 'doubling' of the equations and parameters used in Eq. (14.7). As discussed above, however, this would add quite a bit of complexity without necessarily providing new insight.

Which range of values for a single parameter does result in oscillations depends on the values of the other parameters. Keeping all other parameters as in Fig. 14.4, no oscillations are observed at v_{in}=0.2 (rather than v_{in}=1). However, there are oscillations at v_{in}=0.2 if k_{eri} is increased to 15.7 *and* K is decreased to 1; neither an increase of k_{eri} to 15.7 alone or a decrease of K to 1 alone is sufficient for oscillations. Obviously, it is impossible to predict which parameter values will result in oscillation and which will not. With a software package such as Mathematica©, it is easy to solve Eq. (14.7) numerically for a variety of parameter sets but, for a more systematic study, a stability analysis should be performed. This is done by calculating the so-called eigenvalues for different parameter sets, with positive eigenvalues indicating stable oscillations. For an excellent introduction of the concept of a stability analysis, the reader is referred to Stucki and Somogyi (1994).

For a more informal approach, there are some basic requirements for stable oscillations – as mentioned above – that have to be fulfilled. A system with at least two variables is needed for simple oscillations; three or more are required for bursting or chaotic Ca_{cy} dynamics (Schuster et al. 2002). At least one feedback connection between the oscillating variables as well as 'sufficient total nonlinearity' are required (Stucki and Somogyi 1994). Frequently, this nonlinearity results partly from the nonlinear feedback between the variables; typical elements here are cooperative binding or Michaelis-Menten-type binding. Obviously, for a Ca^{2+} oscillator – a system that is able to produce stable Ca^{2+} oscillations – this needs more than only a Ca^{2+} pump and a Ca^{2+} channel (Harper 2001).

Could the mathematical model of Ca^{2+} oscillations described here for the unicellular green alga *E. viridis* be used to describe Ca^{2+} oscillations in other plant cells? Most likely, yes – with some modifications, of course. In a pharmacological study of Nod factor-induced Ca^{2+} oscillations in root hairs of *Medicago truncatula* (Engstrom et al. 2002), the ER Ca^{2+}-ATPase blockers DBHQ or CPA effectively inhibited Ca^{2+} oscillations at µmolar concentrations – as in *E. viridis*. Caffeine and 2-APB (2-aminoethoxydiphenylborate), modulators of ryanodine receptor and/or IP_3 receptor Ca^{2+} channels, inhibited Nod factor-induced Ca^{2+} oscillations, too (Engstrom et al. 2002). This indicates that, comparably to the model presented here, the second variable might be Ca_{er} or the Ca^{2+} concentration of the nuclear envelope, since Nod factor-induced Ca^{2+} oscillations were shown to initiate in the nuclear region of root hair cells (Ehrhardt et al. 1996). On the other hand, externally applied La^{3+} or Gd^{3+} (1 mM) had no apparent effects on Nod factor-induced Ca^{2+} oscillations (Engstrom et al. 2002), indicating that a model with constant total cellular Ca^{2+} content (v_{in}=0, v_{out}=0) might be more appropriate.

The most attractive system for modelling Ca^{2+} oscillations in plants seems to be stomatal guard cells. Guard cells are the most extensively studied system dealing with the generation of Ca^{2+} oscillations in plant cells (see Sect. 14.2). A variety of stimuli – including ABA, external Ca^{2+}, cold and H_2O_2 – can induce Ca^{2+} oscillations in guard cells, and there is good evidence that different

molecular mechanisms are involved in Ca^{2+} oscillations induced by different stimuli (Allen et al. 2000; Evans et al. 2001; Hetherington and Brownlee 2004). Mathematical modelling should help to clarify the different pathways that are available in guard cells to generate Ca^{2+} oscillations.

Moreover, Ca^{2+} oscillations in guard cells show different shapes and complexities. In *Commelina communis* guard cells (McAinsh et al. 1995), 0.1 mM external Ca^{2+} (Ca_{ext}) induces simple, regular Ca^{2+} oscillations (called symmetrical oscillations by McAinsh et al.) whereas 1.0 mM Ca_{ext} induces bursting oscillations (called asymmetrical oscillations by McAinsh et al.). These issues are described in detail by McAinsh in Chapter 7 of this book. 'Bursting' describes a pattern in which phases of high-frequency oscillations are separated by phases of quiescence and, in Ca^{2+} bursting, usually each phase of oscillation – or each burst – consists of an initial large spike followed by a series of smaller spikes. Simple oscillations, also called regular spiking, can be modelled by relatively simple models with two variables and are often based on CICR – like the model developed above (Eq. 14.7). Bursting oscillations, whether regular or chaotic, require more complex mathematical models with at least three variables and three differential equations (Borghans et al. 1997; Schuster et al. 2002). Mathematical modelling of the transition from simple to bursting Ca^{2+} oscillations at increasing Ca_{ext} in *C. communis* guard cells might give new insight into the molecular mechanisms generating those Ca^{2+} oscillations.

Ca^{2+} influx across the plasma membrane (v_{in} in Fig. 14.1) has been shown to be involved in the generation of Ca^{2+} oscillations in guard cells of different species and under different stimuli (McAinsh et al. 1995; Klüsener et al. 2002). Hyperpolarization-activated plasma membrane Ca^{2+} channels (Hamilton et al. 2000; Pei et al. 2000) seem to play a key role in Ca^{2+} influx into guard cells. This indicates that, in a mathematical model of guard cell Ca^{2+} oscillations, the membrane potential has to be introduced as a separate variable. In experiments with *Vicia faba* guard cells, oscillations in the potential of the guard cell plasma membrane were accompanied by Ca_{cy} transients (Grabov and Blatt 1998). Artificial hyperpolarization of the guard cell plasma membrane results in an increase of Ca_{cy} (Grabov and Blatt 1998; Allen et al. 2000). Accordingly, a mathematical model for regular Ca^{2+} oscillations in guard cells may be based on two variables – Ca_{cy} and the plasma membrane potential. What is the evidence for feedback between these two variables? The membrane potential regulates Ca^{2+} influx in a nonlinear manner. Increasing Ca_{ext} seems to stimulate the opening of hyperpolarization-activated plasma membrane Ca^{2+} channels whereas increasing Ca_{cy} reduces their activity (Hamilton et al. 2000). The Ca^{2+} influx (v_{in}) affects the membrane potential directly whereas increasing Ca_{cy} affects the membrane potential indirectly by regulating different plasma membrane ion channels. In a mathematical model of guard cell Ca^{2+} oscillations, hyperpolarization-activated Ca^{2+} channels would be a central element. They connect the two variables – Ca_{cy} and membrane potential – and, in addition to being regulated by Ca_{cy} and Ca_{ext}, they seem to

be the target of a multitude of signalling pathways that are involved in stomatal closure (Klüsener et al. 2002; Hetherington and Brownlee 2004).

In addition to Ca^{2+} influx across the plasma membrane, there are good indications that Ca^{2+} release from intracellular stores contributes to the generation of Ca^{2+} oscillations in guard cells. A phospholipase C blocker inhibits ABA-induced Ca^{2+} oscillations (Staxen et al. 1999; Klüsener et al. 2002), indicating the importance of intracellular Ca^{2+} release via IP_3 receptor Ca^{2+} channels. Although there is no experimental evidence indicating which intracellular Ca^{2+} store might carry these IP_3 receptors, it seems justified to speculate that oscillations in the Ca^{2+} concentration of a Ca^{2+} store (such as Ca_{er} in Eq. 14.7) can be involved in guard cell Ca^{2+} oscillations – as in many other systems. With three oscillating variables, Ca_{cy}, Ca_{er} (or another store) and the membrane potential, different models for regular Ca^{2+} oscillations can be developed, and even bursting Ca^{2+} oscillations in guard cells might eventually be described by a plausible mathematical model.

Ca^{2+} oscillations in plant cells are a fascinating but not very well-understood phenomenon. One reason for this paucity of information is the complex nature of the oscillations. There is good evidence that, as in animal cells, Ca^{2+} oscillations in plant cells are involved in intracellular signal transduction processes, and that the frequency and amplitude of these oscillations might encode the information to be transmitted (Ng and McAinsh 2003; Hetherington and Brownlee 2004). This means that different stimuli cause Ca^{2+} oscillations of different frequencies and amplitudes and, depending on frequency and amplitude, different physiological reactions are triggered, enabling stimulus-specific reactions. Yet, the encoding mechanisms setting frequency and amplitude remain elusive. There is good experimental evidence on which molecular components might be involved in the generation of intracellular Ca^{2+} oscillations (see Sect. 14.2). However, how these components bring about an oscillation with a certain frequency and amplitude is not understood, and can probably not be without mathematical modelling.

The best way to make reasonable predictions about the frequency and amplitude of a Ca^{2+} oscillation is on the basis of a mathematical model. Theoretical predictions based on mathematical modelling can then be tested experimentally to refine the mathematical model and to improve our understanding of the physiological functions of Ca^{2+} oscillations.

References

Allen GJ, Muir SR, Sanders D (1995) Release of Ca^{2+} from individual plant vacuoles by both $InsP_3$ and cyclic ADP-ribose. Science 268:735–737

Allen GJ, Chu SP, Schumacher K, Shimazaki CT, Vafeados D, Kemper A, Hawke SD, Tallman G, Tsien RY, Harper JF, Chory J, Schroeder JI (2000) Alteration of stimulus-specific guard cell calcium oscillations and stomatal closing in *Arabidopsis det3* mutant. Science 289:2338–2342

Bauer CS, Plieth C, Hansen U-P, Sattelmacher B, Simonis W, Schönknecht G (1997) Repetitive Ca^{2+} spikes in a unicellular green alga. FEBS Lett 405:390–393

Bauer CS, Plieth C, Bethmann B, Popescu O, Hansen U-P, Simonis W, Schönknecht G (1998a) Strontium-induced repetitive calcium spikes in a unicellular green alga. Plant Physiol 117:545–557

Bauer CS, Plieth C, Hansen U-P, Simonis W, Schönknecht G (1998b) A steep Ca^{2+}-dependence of a K^+ channel in a unicellular green alga. J Exp Bot 49:1761–1765

Berridge MJ (1990) Calcium oscillations. J Biol Chem 265:9583–9586

Berridge MJ (1997) The AM and FM of calcium signalling. Nature 386:759–760

Bethmann B, Thaler M, Simonis W, Schönknecht G (1995) Electrochemical potential gradients of H^+, K^+, Ca^{2+}, and Cl^- across the tonoplast of the green alga *Eremosphaera viridis*. Plant Physiol 109:1317–1326

Bootman MD, Young KW, Young JM, Moreton RB, Berridge MJ (1996) Extracellular calcium concentration controls the frequency of intracellular calcium spiking independently of inositol 1,4,5-trisphosphate production in HeLa cells. Biochem J 314:347–354

Borghans J, Dupont G, Goldbeter A (1997) Complex intracellular calcium oscillations A theoretical exploration of possible mechanisms. Biophys Chem 66:25–41

Demaurex N, Lew DP, Krause K-H (1992) Cyclopiazonic acid depletes intracellular Ca^{2+} stores and activates an influx pathway for divalent cations in HL-60 cells. J Biol Chem 267:2318–2324

Dupont G, Goldbeter A (1993) One-pool model for Ca^{2+} oscillations involving Ca^{2+} and inositol 1,4,5-trisphosphate as co-agonists for Ca^{2+} release. Cell Calcium 14:311–322

Dupont G, Berridge MJ, Goldbeter A (1990) Latency correlates with period in a model for signal-induced Ca^{2+} oscillations based on Ca^{2+}-induced Ca^{2+} release. Cell Regul 1:853–861

Ehrhardt DW, Wais R, Long SR (1996) Calcium spiking in plant root hairs responding to *Rhizobium* nodulation signals. Cell 85:673–681

Ehrlich BE, Kaftan E, Bezprozvannaya S, Bezprozvanny I (1994) The pharmacology of intracellular Ca^{2+}-release channels. Trends Pharmacol Sci 15:145–149

Engstrom EM, Ehrhardt DW, Mitra RM, Long SR (2002) Pharmacological analysis of Nod factor-induced calcium spiking in *Medicago truncatula*. Evidence for the requirement of type IIA calcium pumps and phosphoinositide signaling. Plant Physiol 128:1390–1401

Evans NH, McAinsh MR, Hetherington AM (2001) Calcium oscillations in higher plants. Curr Opin Plant Biol 4:415–420

Förster B (1990) Injected inositol 1,4,5-trisphosphate activates Ca^{2+}-sensitive K^+ channels in the plasmalemma of *Eremosphaera viridis*. FEBS Lett 269:197–201

Grabov A, Blatt MR (1998) Membrane voltage initiates Ca^{2+} waves and potentiates Ca^{2+} increases with abscisic acid in stomatal guard cells. Proc Natl Acad Sci USA 95:4778–4783

Gradmann D (2001) Models for oscillations in plants. Austral J Plant Physiol 28:577–590

Hamilton DWA, Hills A, Kohler B, Blatt MR (2000) Ca^{2+} channels at the plasma membrane of stomatal guard cells are activated by hyperpolarization and abscisic acid. Proc Natl Acad Sci USA 97:4967–4972

Harper JF (2001) Dissecting calcium oscillators in plant cells. Trends Plant Sci 6:395–397

Hetherington AM, Brownlee C (2004) The generation of Ca^{2+} signals in plants. Annu Rev Plant Biol 55:401–427

Hwang I, Ratterman DM, Sze H (1997) Distinction between endoplasmic reticulum-type and plasma membrane-type Ca^{2+} pumps. Partial purification of a 120-kilodalton Ca^{2+}-ATPase from endomembranes. Plant Physiol 113:535–548

Inesi G, Sagara Y (1994) Specific inhibitors of intracellular Ca^{2+} transport ATPases. J Membr Biol 141:1–6

Kass GEN, Duddy SK, Moore GA, Orrenius S (1989) 2,5-Di-(*tert*-butyl)-1,4-benzohydroquinone rapidly elevates cytosolic Ca^{2+} concentration by mobilizing the inositol 1,4,5-trisphosphate-sensitive Ca^{2+} pool. J Biol Chem 264:15192–15198

Klüsener B, Young JJ, Murata Y, Allen GJ, Mori IC, Hugouvieux V, Schroeder JI (2002) Convergence of calcium signaling pathways of pathogenic elicitors and abscisic acid in *Arabidopsis* guard cells. Plant Physiol 130:2152–2163

Kraus M, Wolf B, Wolf B (1996) Crosstalk between cellular morphology and calcium oscillation patterns. Insights from a stochastic computer model. Cell Calcium 19:461–472

Kummer U, Krajnc B, Pahle J, Green AK, Dixon CJ, Marhl M (2005) Transition from stochastic to deterministic behavior in calcium oscillations. Biophys J 89:1603–1611

Liang F, Cunningham KW, Harper JF, Sze H (1997) ECA1 complements yeast mutants defective in Ca^{2+} pumps and encodes an endoplasmic reticulum-type Ca^{2+}-ATPase in *Arabidopsis thaliana*. Proc Natl Acad Sci USA 94:8579–8584

Logan DC, Venis MA (1995) Characterisation and immunological identification of a calmodulin-stimulated Ca^{2+}-ATPase from maize shoots. J Plant Physiol 145:702–710

Ma J (1993) Block by ruthenium red of the ryanodine-activated calcium release channel of skeletal muscle. J Gen Physiol 102:1031–1056

McAinsh MR, Webb AAR, Taylor JE, Hetherington AM (1995) Stimulus-induced oscillations in guard cell cytosolic free calcium. Plant Cell 7:1207–1219

Meissner G (1994) Ryanodine receptor/Ca^{2+} release channels and their regulation by endogenous effectors. Annu Rev Physiol 56:485–508

Meissner G, Darling E, Eveleth J (1986) Kinetics of rapid calcium release by sarcoplasmic reticulum. Effects of calcium, magnesium, and adenine nucleotides. Biochemistry 25:236–244

Meyer T, Stryer L (1988) Molecular model for receptor-stimulated calcium spiking. Proc Natl Acad Sci USA 85:5051–5055

Muir SR, Sanders D (1996) Pharmacology of Ca^{2+} release from red beet microsomes suggests the presence of ryanodine receptor homologs in higher plants. FEBS Lett 395:39–42

Ng CKY, McAinsh MR (2003) Encoding specificity in plant calcium signalling: hot-spotting the ups and downs and waves. Ann Bot 92:477–485

Pei Z-M, Murata Y, Benning G, Thomine S, Klüsener B, Allen GJ, Grill E, Schroeder JI (2000) Calcium channels activated by hydrogen peroxide mediate abscisic acid signalling in guard cells. Nature 406:731–734

Pessah IN, Stambuk RA, Casida JE (1987) Ca^{2+}-activated ryanodine binding: mechanisms of sensitivity and intensity modulation by Mg^{2+}, caffeine, and adenine nucleotides. Mol Pharmacol 31:232–238

Schönknecht G, Bethmann B (1998) Cytosolic Ca^{2+} and H^+ buffers in green algae: a comment. Protoplasma 203:206–209

Schuster S, Marhl M, Hofer T (2002) Modelling of simple and complex calcium oscillations: from single-cell responses to intercellular signalling. Eur J Biochem 269:1333–1355

Shabala S, Shabala L, Gradmann D, Chen Z, Newman I, Mancuso S (2006) Oscillations in plant membrane transport: model predictions, experimental validation, and physiological implications. J Exp Bot 57:171–184

Smith JS, Imagawa T, Ma J, Fill M, Campbell KP, Coronado R (1988) Purified ryanodine receptor from rabbit skeletal muscle is the calcium-release channel of sarcoplasmic reticulum. J Gen Physiol 92:1–26

Somogyi R, Stucki JW (1991) Hormone-induced calcium oscillations in liver cells can be explained by a simple one pool model. J Biol Chem 266:11068–11077

Staxen I, Pical C, Montgomery LT, Gray JE, Hetherington AM, McAinsh MR (1999) Abscisic acid induces oscillations in guard-cell cytosolic free calcium that involve phosphoinositide-specific phospholipase C. Proc Natl Acad Sci USA 96:1779–1784

Stucki JW, Somogyi R (1994) A dialogue on Ca^{2+} oscillations: an attempt to understand the essentials of mechanisms leading to hormone-induced intracellular Ca^{2+} oscillations in various kinds of cells on a theoretical level. Biochim Biophys Acta 1183:453–472